

## New candidate for deformed halo nucleus in Mg isotopes through analysis of reaction cross sections

S. Watanabe<sup>1,a</sup>, K. Minomo<sup>1</sup>, S. Tagami<sup>1</sup>, M. Shimada<sup>1</sup>, M. Kimura<sup>2</sup>, M. Takechi<sup>3,4</sup>, M. Fukuda<sup>5</sup>, D. Nishimura<sup>6</sup>, T. Suzuki<sup>7</sup>, T. Matsumoto<sup>1</sup>, Y. R. Shimizu<sup>1</sup>, and M. Yahiro<sup>1</sup>

<sup>1</sup>Department of Physics, Kyushu University, Fukuoka 812-8581, Japan

<sup>2</sup>Creative Research Institution (CRIS), Hokkaido University, Sapporo 001-0021, Japan

<sup>3</sup>Gesellschaft für Schwerionenforschung GSI, 64291 Darmstadt, Germany

<sup>4</sup>RIKEN, Nishina Center, Wako, Saitama 351-0106, Japan

<sup>5</sup>Department of Physics, Osaka University, Osaka 560-0043, Japan

<sup>6</sup>Department of Physics, Tokyo University of Science, Tokyo, 278-8510, Japan

<sup>7</sup>Department of Physics, Saitama University, Saitama 338-8570, Japan

**Abstract.** The total reaction cross sections of Mg isotopes on a  $^{12}\text{C}$  target at 240 MeV/nucleon have been analyzed with a fully microscopic framework, i.e., the double folding model with the density calculated by antisymmetrized molecular dynamics. Our results well reproduce the latest experimental data except  $^{37}\text{Mg}$  as a new candidate for a deformed halo nucleus.

### 1 Introduction

The Radioactive Ion Beam Factory (RIBF) at RIKEN has added a new page to the history of the study of unstable nuclei. It has enabled us to reach unstable nuclei very far from the line of  $\beta$ -stability experimentally. One of the most attractive region is the island of inversion ( $Z \sim 10\text{--}12$ ,  $N \sim 20\text{--}22$ ), and nuclei in the region have low excitation energies and large  $B(E2)$  values, reflecting strong deformation. When a nucleus is deformed, the deformation makes the root mean square (RMS) radius effectively large compared with a spherical nucleus. Hence, this enhances the total reaction cross section  $\sigma_R$ , since  $\sigma_R$  strongly depends on the RMS radii of a projectile and a target,  $\sigma_R \approx \pi(R_P + R_T)^2$ , where  $R_P$  ( $R_T$ ) is the RMS radius of a projectile (target). In fact, large interaction cross sections  $\sigma_I$  which are almost the same as  $\sigma_R$  have been measured for  $^{29\text{--}32}\text{Ne}$  [1, 2]. In particular for  $^{31}\text{Ne}$ , the  $\sigma_I$  is much larger than any other Ne isotopes that was measured. This remarkable behavior has stimulated many research activities [3–6].

In the previous studies [3, 4], the measured cross sections of Ne isotopes on a  $^{12}\text{C}$  target at 240 MeV/nucleon have been analyzed by means of the double folding model (DFM) with the densities calculated by antisymmetrized molecular dynamics (AMD). This model is a fully microscopic framework for calculating  $\sigma_R$ . The model well reproduces the experimental data, and hence it is concluded that  $^{29\text{--}32}\text{Ne}$  have strong deformation and  $^{31}\text{Ne}$  is a deformed halo nucleus; a halo structure with large deformation. It should be noted that  $^{31}\text{Ne}$  is the heaviest halo nucleus experimentally confirmed at this

---

<sup>a</sup>e-mail: s-watanabe@phys.kyushu-u.ac.jp

stage. In this paper, we apply this model to the analysis of the scattering of Mg isotopes and compare the results with the experimental data [7] that have been already measured but not been published yet. Our theoretical results well reproduce the experimental data on  $\sigma_R$  and the structure of  $^{37}\text{Mg}$  is briefly discussed as a new candidate of deformed halo nuclei.

## 2 Theoretical framework

The framework of the theoretical calculation is the same as in Ref. [4]. The optical potential  $U$  is constructed with the DFM from the  $g$ -matrix interaction. As for the  $g$ -matrix interaction, we employ the Melbourne interaction [8] constructed from the Bonn-B nucleon-nucleon potential [9]. The optical potential  $U$  consists of the direct part ( $U^{\text{DR}}$ ) and the exchange part ( $U^{\text{EX}}$ ) defined by

$$U^{\text{DR}}(\mathbf{R}) = \sum_{\mu,\nu} \int \rho_{\text{P}}^{\mu}(\mathbf{r}_{\text{P}}) \rho_{\text{T}}^{\nu}(\mathbf{r}_{\text{T}}) g_{\mu\nu}^{\text{DR}}(s; \rho_{\mu\nu}) d\mathbf{r}_{\text{P}} d\mathbf{r}_{\text{T}}, \quad (1)$$

$$U^{\text{EX}}(\mathbf{R}) = \sum_{\mu,\nu} \int \rho_{\text{P}}^{\mu}(\mathbf{r}_{\text{P}}, \mathbf{r}_{\text{P}} - \mathbf{s}) \rho_{\text{T}}^{\nu}(\mathbf{r}_{\text{T}}, \mathbf{r}_{\text{T}} + \mathbf{s}) g_{\mu\nu}^{\text{EX}}(s; \rho_{\mu\nu}) \exp[-i\mathbf{K}(\mathbf{R}) \cdot \mathbf{s}/M] d\mathbf{r}_{\text{P}} d\mathbf{r}_{\text{T}}, \quad (2)$$

where  $\mathbf{s} = \mathbf{r}_{\text{P}} - \mathbf{r}_{\text{T}} + \mathbf{R}$  for the coordinate  $\mathbf{R}$  between P and T. The coordinate  $\mathbf{r}_{\text{P}}$  ( $\mathbf{r}_{\text{T}}$ ) denotes the location of the interacting nucleon measured from the center-of-mass of the projectile (target). Each of  $\mu$  and  $\nu$  stands for the  $z$ -component of isospin;  $1/2$  means neutron and  $-1/2$  does proton. The original form of  $U^{\text{EX}}$  is a non-local function of  $\mathbf{R}$ , but it has been localized in Eq. (2) with the local semi-classical approximation in which P is assumed to propagate as a plane wave with the local momentum  $\hbar\mathbf{K}(\mathbf{R})$  within a short range of the nucleon-nucleon interaction, where  $M = AA_{\text{T}}/(A+A_{\text{T}})$  for the mass number  $A$  ( $A_{\text{T}}$ ) of P (T). The validity of this localization is shown in Ref. [3].

In order to construct the densities in Eqs. (1) and (2), we employ AMD [10] with the Gogny D1S force. The variational wave function is a parity-projected wave function and the intrinsic wave function is a Slater determinant of nucleon wave packets,

$$\Phi^{\pi} = P^{\pi} \mathcal{A} \{ \varphi_1, \varphi_2, \dots, \varphi_A \}, \quad \varphi_i = \phi_i(\mathbf{r}) \chi_i \xi_i, \quad (3)$$

where  $P^{\pi}$  is the parity projector. The  $i$ -th single wave packet  $\varphi_i$  consists of spatial  $\phi_i$ , spin  $\chi_i$ , and isospin  $\xi_i$  parts. The variational parameters in Eq. (3) are determined by using the frictional cooling method to minimize the total energy under the constraint on the matter quadrupole deformation parameter  $\beta$ . We then obtain the optimal wave function  $\Phi^{\pi}(\beta)$  for a given value of  $\beta$ . Note that we never make any assumption on the spatial symmetry of the wave function in this calculation. After that, we do the angular momentum projection for each value of  $\beta$ . Finally, we perform the generator coordinate method and superpose all of the wave functions that have the same parity and angular momentum. In the DFM calculation, the ground state wave function obtained here is transformed to the proton and neutron densities, and only the spherical parts of the densities are taken. Although this approximation makes the double-folding potential spherical, it is quite good as shown in Ref. [4].

## 3 Results

First, we apply the DFM to the analysis of the reaction of stable nuclei in order to confirm the accuracy of the model for the intermediate energy of 240 MeV/nucleon. For the test,  $^{12}\text{C}$  scattering on the stable targets  $^{12}\text{C}$ ,  $^{20}\text{Ne}$ ,  $^{23}\text{Na}$  and  $^{27}\text{Al}$  at around 250 MeV/nucleon are taken. We employ the phenomenological densities as the ones of these stable nuclei in the DFM. The proton distribution

is deduced from electron scattering and the neutron distribution is assumed to have the same geometry as the proton one. This assumption gives a good description for the present interest of the  $\sigma_R$ , because the neutron RMS radii are almost the same as the proton ones for these stable nuclei in the Hartree-Fock calculations.

Figure 1 (a) shows  $\sigma_R$  for  $^{12}\text{C}$ ,  $^{20}\text{Ne}$ ,  $^{23}\text{Na}$  and  $^{27}\text{Al}$  targets. The experimental data are taken from Refs. [11–13]. The dotted line represents the original results of DFM calculations. The results well reproduce the experimental data overall, but they slightly overestimate the data. Here, we introduce the normalization parameter of  $F = 0.982$  to reproduce the mean value of the experimental data for  $^{12}\text{C}$ . Then we have the solid curve, that is consistent with all the experimental data. This procedure is just a fine tuning, so we never change the factor in the following.

In Refs. [3, 4], the DFM was applied to the analysis of  $\sigma_R$  for the scattering of Ne isotopes on  $^{12}\text{C}$  at 240 MeV/nucleon as shown in Fig. 1 (b). The solid curve represents the results with AMD densities and it is in excellent agreement with all the experimental data except for  $^{31}\text{Ne}$ . The underestimation may come mainly from the inaccuracy of the AMD density in its tail region. This is seen when a nucleus extremely extends, i.e., for halo nucleus. However, this discrepancy was solved by the tail correction with the resonating group method (RGM). This result indicates that the accurate tail description is necessary for the  $^{31}\text{Ne}$  density in order to explain the large interaction cross section. Thus, the  $\sigma_R$  of Ne isotopes have been well described by the DFM with the AMD densities.

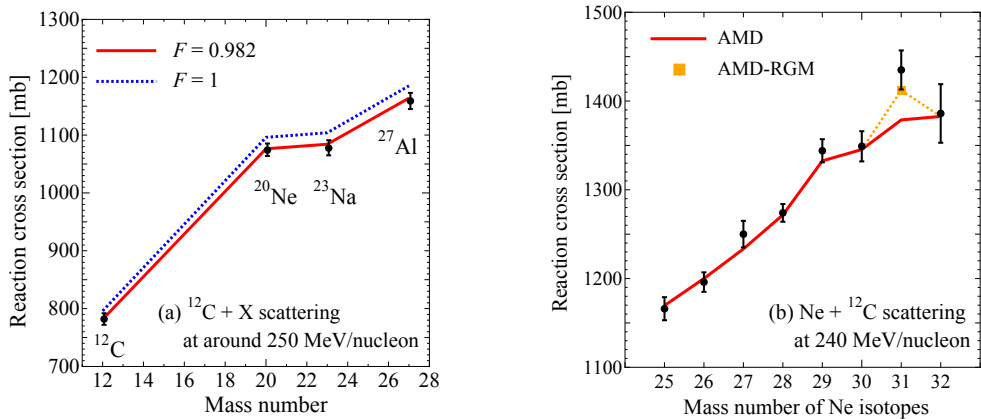


**Figure 1.** (Color online) (a) Reaction cross sections for the scattering of  $^{12}\text{C}$  on stable nuclei;  $^{12}\text{C}$ ,  $^{20}\text{Ne}$ ,  $^{23}\text{Na}$ , and  $^{27}\text{Al}$ . The solid (dotted) line stands for the results of DFM calculations with (without) the normalization parameter  $F = 0.982$ . The experimental data are taken from Refs. [11–13]. (b) Reaction cross sections for the scattering of Ne isotopes on  $^{12}\text{C}$  at 240 MeV/nucleon. The solid line represents the results of the AMD calculations. The closed square is the AMD calculation with the tail corrections for  $^{31}\text{Ne}$ .

Now, we apply the DFM to the analysis of Mg isotopes. The reaction cross sections are shown in Fig. 2 for the scattering of Mg isotopes on  $^{12}\text{C}$  at 240 MeV/nucleon. The solid line with closed circles denotes the results of AMD densities. Since the experimental data are not published yet, we only show the theoretical results, but they well reproduce the experimental data overall just as the case of Ne isotopes. Here, we comment only on the reaction cross section of  $^{37}\text{Mg}$ .  $^{37}\text{Mg}$  is a new candidate of deformed halo nuclei since the separation energy is estimated to be small ( $\sim 250$  keV [14],  $\sim 162$  keV [15]). In fact, the experimental datum on  $\sigma_R$  for  $^{37}\text{Mg}$  is large, but our theoretical result is not. This situation suggests that we need to perform the AMD-RGM calculation for the tail correction. It is

expected that  $^{37}\text{Mg}$  is a deformed halo nucleus, and a situation similar to the case of  $^{31}\text{Ne}$  occurs. This point will be discussed in a forthcoming paper through the direct comparison with the experimental data.

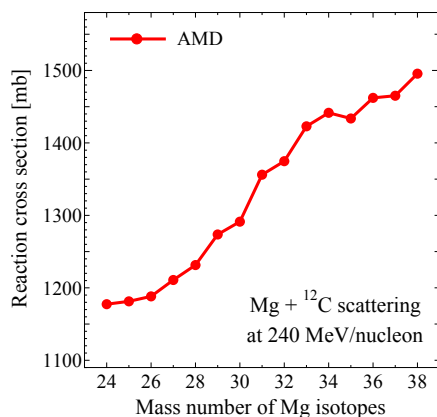


**Figure 2.** (Color online) Reaction cross sections for the scattering of Mg isotopes on  $^{12}\text{C}$  at 240 MeV/nucleon. The solid line with closed circles represents the results of the AMD calculations.

## 4 Summary

We have investigated the total reaction cross sections of Mg isotopes at 240 MeV/nucleon by means of the DFM with the AMD densities. Our results well reproduce the experimental data overall except for  $^{37}\text{Mg}$ . This situation is very similar to the case of  $^{31}\text{Ne}$ , and it suggests that further analyses including the tail correction should be made. We will discuss this point in a forthcoming paper.

## References

- [1] M. Takechi *et al.*, Nucl. Phys. A **834**, 412c (2010).
- [2] M. Takechi *et al.*, Phys. Lett. B **707**, 357 (2012).
- [3] K. Minomo *et al.*, Phys. Rev. Lett. **108**, 052503 (2012).
- [4] T. Sumi *et al.*, Phys. Rev. C **85**, 064613 (2012).
- [5] W. Horiuchi *et al.*, Phys. Rev. C **86**, 024614 (2012).
- [6] Y. Urata *et al.*, Phys. Rev. C **86**, 044613 (2012).
- [7] M. Takechi and M. Fukuda, private communication.
- [8] K. Amos, P. J. Dortmans, H. V. von Geramb, S. Karataglidis, and J. Raynal, in *Advances in Nuclear Physics*, edited by J. W. Negele and E. Vogt (Plenum, New York, 2000) Vol. 25, p. 275.
- [9] R. Machleidt *et al.*, Phys. Rep. **149**, 1(1987).
- [10] M. Kimura, Phys. Rev. C **75**, 041302 (2007).
- [11] M. Takechi, *et al.*, Phys. Rev. C **79**, 061601(R) (2009).
- [12] L. Chulkov *et al.*, Nucl. Phys. A **603** 219, (1996).
- [13] T. Suzuki *et al.*, Phys. Rev. Lett. **75**, 3241 (1995).
- [14] G. Audi *et al.*, Nucl. Phys. A **729** 337, (2003).
- [15] J. Cameron *et al.*, Nucl. Data. Sheets. **113**, 365 (2012).